Mathematical modeling and analysis of a Generalized Unified Power Flow Controller with Device rating Methodology

Chintalapudi Venkata Suresh and Sirigiri Sivanaga Raju

Department of Electrical & Electronics Engineering, UCEK, JNTU Kakinada,
Kakinada, A.P., India, 533 003.
venkatasuresh3@gmail.com and sirigiri70@yahoo.co.in

Abstract: Ever incrasing demand on power system needs latest FACTS devices to increase the power transfer capability. One of such device is Generalized Unified Power Flow Controller. This device has got more emphasis, as it has five/more degree of freedom, it can simultaneously control the voltage at the sending end and the power flow through the transmission lines to which the device is connected. The detailed Power Injection Model (PIM) of GUPFC is proposed in this paper. Location and rating of the device plays a major role, to get proper control in power system. An optimal placement strategy based on single line contingencies through performance index is proposed. Without loss of generality, device rating is calculated based on the power handling capacity of the converters. Series and Shunt Converter switching losses and the shunt converter reactive power injection are considered, to analyze the effect of the device. Analytical results confirms the effect of the device control parameters on a given test system.

Keywords: Generalized Unified Power Flow Controller, Power Injection Model, Performance Index, Contingency Analysis, FACTS device rating.

1. Introduction

Flexible AC Transmission Systems (FACTS) has got good reputation because of getting higher controllability and increasing power transfer capability by means of power electronic based converters [1]. Basically these devices reduce the network expansion cost/transmission lines installation cost, by properly managing the system parameters. The basic applications of the FACTS devices are: power flow control, increase of transmission capability, voltage control, reactive power compensation, stability improvement, power quality improvement, etc [2]. It can be seen that with the growing demand for electricity, the opportunity for FACTS-devices gets more and more important.

The Unified Power Flow Controller (UPFC) can be used for simultaneous control of the power system parameters (voltage, impedance, phase angle), or any of the above combinations [3, 4]. A comprehensive load flow model for UPFC, to incorporate into existing Newton-Raphson (NR) Load flow is presented in [5]. An algorithm is proposed for determining the optimum flow and size of UPFC for power flow applications [6]. The UPFC operation, control, sequencing, and protection methodologies under practical constraints are discussed in [7]. An effective modeling of UPFC and its performance has been presented in [8, 9]. A set of analytical equations are derived to control any combination of the power system parameters or none of them [10]. It is possible to study the power flow control in the presence of UPFC by obtaining sensitivity matrix of the power system[11]. The congestion management in power system is possible with the selection of suitable location and settings of its control parameters[12]. An effective injection modeling approaches to power flow analysis in the presence of UPFC is discussed in [13-15]. Power Injection Model (PIM) of UPFC and its effect, based on location are analyzed in [16, 17]. Advanced UPFC model to reuse NR Load flow has been developed in [18].

It is possible to extend the concept of voltage and power flow control beyond what is achievable with the UPFC; name of the device is Generalized Unified Power Flow Controller (GUPFC). Figure 1 shows the principle configuration of the GUPFC. Simply, it consists of

Received: September 9th, 2014. Accepted: March 7th, 2015
DOI: 10.15676/ijeei.2015.7.1.5

three converters, one connected in shunt and the other two are in series with two transmission lines at a bus. This basic configuration can control total five power system quantities such as a bus voltage and independent active and reactive power flow in two lines.

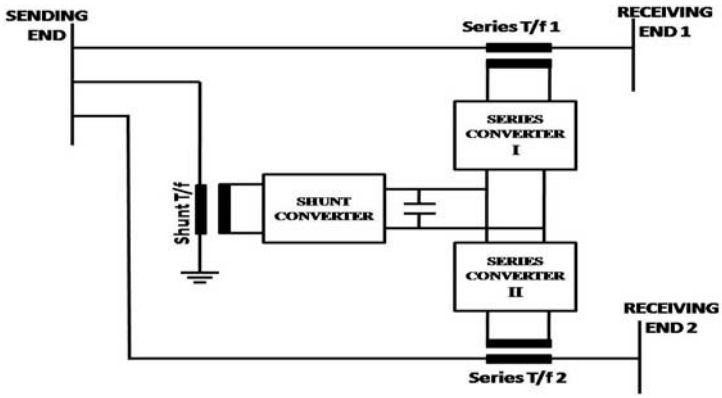

Figure 1. Principle configuration of GUPFC

The complete working procedure and fundamental frequency model of GUPFC is described in [19]. In [20], a mathematical model of the GUPFC suitable for power flow is proposed. Voltage source based mathematical models of the GUPFC and its implementation in Newton power flow is presented in [21]. In [22], the application of GUPFC in a real power grid for power flow as well as voltage control by applying a four converter GUPFC in Sichuan power system of China is analyzed. Steady state mathematical model of GUPFC, based on d-q axis reference frame decomposition has been derived in [23]. Robust modeling of the GUPFC with small impedances in power flow analysis is given in [24]. A fuzzy rule based model for GUPFC is proposed in [25]. Nonlinear predictor-corrector primal-dual interior-point optimal power flow algorithm for GUPFC is presented in [26]. The design of the GUPFC damping controller is designed in [27]. Analysis of sub synchronous resonance with GUPFC is presented in [28].

The concept of GUPFC can be extended for more lines, if necessary. By using GUPFC devices, the transfer capability of transmission lines can be increased significantly. Further mores, by using the multi-line management capability of GUPFC; active power flows on lines can not only be increased, but also be decreased with respect to operating and market transaction requirement [24]. From the careful review of the literature, it is identified that, in the GUPFC modeling, the switching converter losses are not considered.

In this paper, the main contribution is to develop Power Injection Model (PIM) of GUPFC with converter switching losses to get an effective control and secured operation. A proper location to install the device is calculated by using single line contingency analysis. An optimal rating of the device is estimated without loss of generality i.e. by using power handling capability of the device subjected to the system loading conditions. The main advantage of the proposed methodology is that, the rating and the optimal location of GUPFC are obtained to show the effectiveness of the device on system parameters, which is not available in the existing literature. The efficiency of the proposed model is tested on Hale Network.

A. Critic on Literature

Most of the literature has not given the detailed mathematical PIM of GUPFC in an optimal location with proper size to analyze the effect of the same on a given power system. So, there is a need of such a stated modeling to get proper control over the network to optimize certain objectives. Hence in this paper, optimal location finding strategy, proper device size calculation strategy, and a detailed analysis of the GUPFC power injection model are presented.

2. Operating principle of GUPFC

There are several possibilities of operating configurations by combining two or more converter blocks with flexibility. The GUPFC with combining three or more three-phase switching converters connected back-back through coupling transformers.

The main function of the converter is to change a DC input voltage to a symmetrical AC output voltage of desired magnitude, frequency and phase shift with respect to the selected reference. The function of coupling transformers is to isolate GUPFC and transmission line and to match the voltage levels between the line and the voltage produced by the converters. Series converter inserts voltage of controllable magnitude and controllable phase angle in series with the transmission line via series connected transformer, thereby it provides the control of real and reactive power flow in the transmission line. The real power injected into the system by the series branches must be taken from the parallel branch through dc link. The real power flows in either direction between AC terminals of the converters.

3. GUPFC Mathematical modeling

A GUPFC can be represented by three voltage sources, which are controllable in both magnitude and phase angle and are representing fundamental components of output voltages of three converters & impedances being leakage reactance's of three coupling transformers. Let us define three GUPFC buses i, j and k as shown in Figure 2. The following considerations are taken for analysis purpose:

1. Voltage at bus-i is taken as $\overline{V_i} = V_i \angle \delta_i$
2. The two controllable series injected voltage sources are identical.
3. The leakage reactance of the two series coupling transformers is equal.

The two controllable series voltage sources source $\overline{V}_{se_1}$ and $\overline{V}_{se_2}$ are defined as

$$\overline{V}_{se_1} = \overline{V}_{se_2} = \overline{V}_{se} = rV_i e^{j\gamma} \tag{1}$$

where 'r' and 'γ' are respective per unit magnitude and phase angles of series voltages, and which are operating in the following specified limits

$$0 \le r \le r_{max} \quad \text{and} \quad 0 \le \gamma \le \gamma_{max}$$

The GUPFC device is incorporated in between three GUPFC buses, out of which one is a common bus for the remaining two buses. Briefly, one of the series converters is connected between bus-i and bus-j, similarly, another series converter is connected between bus-i and bus-k. The GUPFC power injection model is developed in two stages, one is series connected voltage source model and the other is shunt connected voltage source model.
The voltages behind the series reactance's can be calculated as

$$\overline{V}'_{ij} = \overline{V_i} + \overline{V}_{se_1} \quad \textit{and} \quad \overline{V}'_{ik} = \overline{V_i} + \overline{V}_{se_2} \tag{2}$$

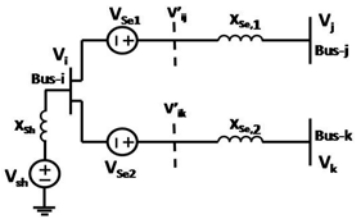

Figure 2. Voltage source model of GUPFC

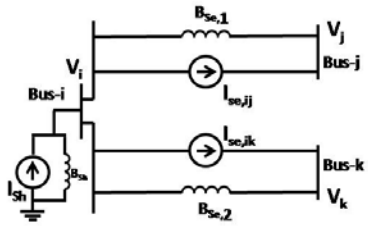

Figure 3. Equivalent current source model of GUPFC

A. Series connected voltage source mode

According to Norton's theorem, the series connected voltage source can be modeled by replacing the voltage source '$\bar{V}_{se}$' with an equivalent current source '$\bar{I}_{se}$' in parallel with a transmission line susceptance 'B_{se}' as shown in figure 3.

where

$$B_{se} = \frac{1}{X_{se}} \tag{3}$$

X_{se} is the series transformer equivalent reactance

The amount of current flowing from the source is given as

$$\bar{I}_{se} = \frac{\bar{V}_{se}}{jX_{se}} = -jB_{se}\bar{V}_{se} \tag{4}$$

replace $\bar{V}_{se}$ in Eq.(4) from Eq.(1)

$$\bar{I}_{se} = -jrV_iB_{se}e^{j(\delta_i+\gamma)} = -rV_iB_{se}e^{j(90^\circ+\delta_i+\gamma)} \tag{5}$$

hence

$$(\bar{I}_{se})^* = -rV_iB_{se}e^{-j(90^\circ+\delta_i+\gamma)} \tag{6}$$

This current source can be modeled by injecting equivalent powers at the respective buses, to which the device is connected. The corresponding power injections are shown in figure.4.

This model can be seen as the three independent complex powers injections at the GUPFC buses and can be written as

$$\bar{S}_{i_{se}} = -2\bar{V}_i(\bar{I}_{se})^* \tag{7}$$

$$\bar{S}_{j_{se}} = \bar{V}_j(\bar{I}_{se})^* \tag{8}$$

$$\bar{S}_{k_{se}} = \bar{V}_k(\bar{I}_{se})^* \tag{9}$$

the detailed expressions for these injections can be deduced by substituting Eq. (6) in Eqs. (7)-(9)

$$\bar{S}_{i_{se}} = 2rV_i^2B_{se}e^{-j(90^\circ+\gamma)}$$

$$\overline{S}_{j_{se}} = -rV_iV_jB_{se}e^{-j(90^\circ+\delta_i-\delta_j+\gamma)}$$

$$\overline{S}_{k_{se}} = -rV_iV_kB_{se}e^{-j(90^\circ+\delta_i-\delta_k+\gamma)}$$

by using Eulers identity, $e^{j\alpha} = \cos\alpha + j\sin\alpha$; let us define $\delta_{ij} = \delta_i - \delta_j$ and $\delta_{ik} = \delta_i - \delta_k$

$$\overline{S}_{i_{se}} = 2rV_i^2B_{se}(\cos(90^\circ+\gamma) - j\sin(90^\circ+\gamma)) \quad (10)$$

$$\overline{S}_{j_{se}} = -rV_iV_jB_{se}(\cos(90^\circ+\delta_{ij}+\gamma) - j\sin(90^\circ+\delta_{ij}+\gamma)) \quad (11)$$

$$\overline{S}_{k_{se}} = -rV_iV_kB_{se}(\cos(90^\circ+\delta_{ik}+\gamma) - j\sin(90^\circ+\delta_{ik}+\gamma)) \quad (12)$$

by using trigonometric identities in Eqs (10)-(12), the active and reactive power injections at i, j, k are

$$P_{i_{se}} = -2rV_i^2B_{se}\sin(\gamma) \quad (13)$$

$$Q_{i_{se}} = -2rV_i^2B_{se}\cos(\gamma) \quad (14)$$

$$P_{j_{se}} = rV_iV_jB_{se}\sin(\delta_{ij}+\gamma) \quad (15)$$

$$Q_{j_{se}} = rV_iV_jB_{se}\cos(\delta_{ij}+\gamma) \quad (16)$$

$$P_{k_{se}} = rV_iV_kB_{se}\sin(\delta_{ik}+\gamma) \quad (17)$$

$$Q_{k_{se}} = rV_iV_kB_{se}\cos(\delta_{ik}+\gamma) \quad (18)$$

The equivalent series connected voltage source model with the corresponding power injections is shown in figure 4.

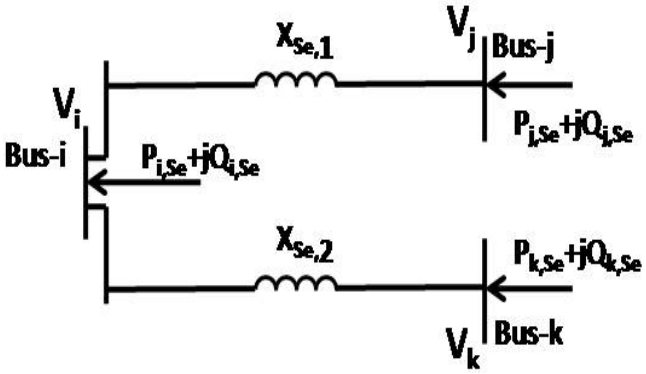

Figure 4. Equivalent series connected voltage source model

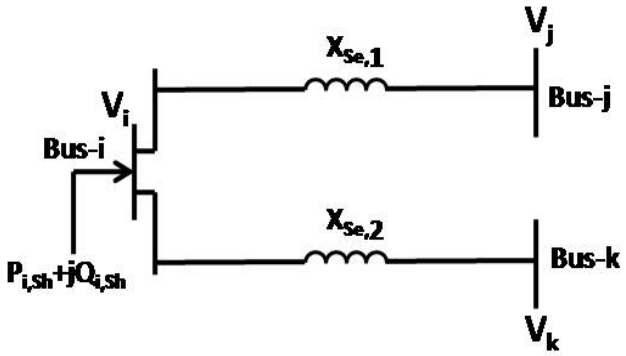

Figure 5. Equivalent shunt connected voltage source model

The amount of apparent power supplied by the two series converters is derived as

$$\overline{S}_{se_1} = P_{se_1} + jQ_{se_1} = \overline{V}_{se}(\overline{I}_{ij})^* = jrV_iB_{se}e^{j(\delta_i+\gamma)}(\overline{V'}_{ij} - \overline{V_j})^* \quad (19)$$

substitute Eq.(2) in Eq.(18) and simplify

$$P_{se_1} + jQ_{se_1} = jrV_iB_{se}e^{j(\delta_i+\gamma)}(rV_ie^{-j(\delta_i+\gamma)} + V_ie^{-j\delta_i} - V_je^{-j\delta_j})$$

$$= jr^2V_i^2B_{se} + jrV_i^2B_{se}(\cos\gamma + j\sin\gamma) - jrV_iV_jB_{se}(\cos(\delta_{ij}+\gamma) + j\sin(\delta_{ij}+\gamma))$$

equate real and imaginary parts, then

$$P_{se_1} = rV_iV_jB_{se}\sin(\delta_{ij}+\gamma) - rV_i^2B_{se}\sin\gamma \quad (20)$$

$$Q_{se_1} = -rV_iV_jB_{se}\cos(\delta_{ij}+\gamma) + rV_i^2B_{se}\cos\gamma + r^2V_i^2B_{se} \quad (21)$$

Similarly,

$$P_{se_2} = rV_iV_kB_{se}\sin(\delta_{ik}+\gamma) - rV_i^2B_{se}\sin\gamma \quad (22)$$

$$Q_{se_2} = -rV_iV_kB_{se}\cos(\delta_{ik}+\gamma) + rV_i^2B_{se}\cos\gamma + r^2V_i^2B_{se} \quad (23)$$

B. Shunt connected voltage source model

The shunt connected voltage source can be modeled as an equivalent power injection from GUPFC shunt branch to the series branches through converters 1 and 2. This model is also used to provide the converter switching losses. The reactive power injection at shunt converter is used to control/maintain the voltage level at sending end within limits. The equivalent shunt connected voltage source model with the corresponding power injections is shown in Figure.5. The total switching losses of the one converter is about 0.8-1% [2,21] of the power transferred through the converter. If these losses are considered, then the real power injection of the shunt converter is

$$P_{sh} = -1.03(P_{se_1} + P_{se_2}) \quad (24)$$

from Eqs.(20) and (22),

$$P_{sh} = 2.06rV_i^2B_{se}\sin\gamma - 1.03rV_iV_jB_{se}\sin(\delta_{ij}+\gamma) - 1.03rV_iV_kB_{se}\sin(\delta_{ik}+\gamma)$$

Assume constant Q_{sh} is injected at bus-i. The apparent power injection at shunt branch is $\overline{S}_{sh} = P_{sh} + jQ_{sh}$.

C. GUPFC mathematical model

The final steady state model of GUPFC power injection model is obtained by combining series connected voltage and shunt connected voltage source models. Then the equivalent GUPFC model is shown in Figure 6. The resultant power injections are given as

$$P_{i,gupfc} = P_{i_{se}} + P_{sh} \tag{25}$$

$$P_{i,gupfc} = 0.06rV_i^2 B_{se} \sin\gamma - 1.03rV_iV_jB_{se}\sin(\delta_{ij}+\gamma) - 1.03rV_iV_kB_{se}\sin(\delta_{ik}+\gamma)$$

$$Q_{i,gupfc} = Q_{i_{se}} + Q_{sh} = -2rV_i^2 B_{se}\cos\gamma + Q_{sh} \tag{26}$$

$$P_{j,gupfc} = P_{j_{se}} = rV_iV_jB_{se}\sin(\delta_{ij}+\gamma) \tag{27}$$

$$Q_{j,gupfc} = Q_{j_{se}} = rV_iV_jB_{se}\cos(\delta_{ij}+\gamma) \tag{28}$$

$$P_{k,gupfc} = P_{k_{se}} = rV_iV_kB_{se}\sin(\delta_{ik}+\gamma) \tag{29}$$

$$Q_{k,gupfc} = Q_{k_{se}} = rV_iV_kB_{se}\cos(\delta_{ik}+\gamma) \tag{30}$$

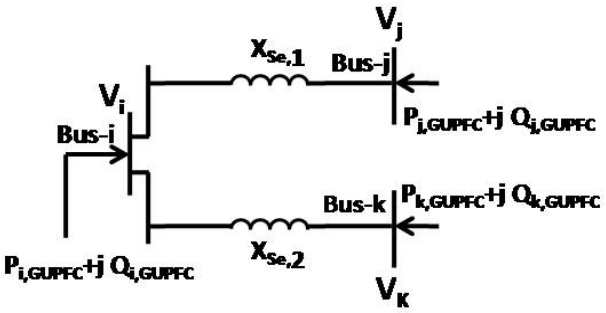

Figure 6. GUPFC mathematical model

D. Computational flow

Initially contingency analysis is performed for a given system to find a place where two lines attached to the critical bus, to install GUPFC. After this the device rating is calculated by using the procedure mentioned in the section 5 and using the flow chart shown in Figure.7. Then, the complete analysis of the effect of GUPFC on a given test system is performed by using NR load flow.

To study the impact of GUPFC on an electrical power network, the device model should be incorporated into the system. Power Injection Model is a popularly used model to incorporate the device by changing the Jacobian and power mismatche equations in Newton-Raphson algorithm[16].

The linearized system model based on NR algorithm is written as,

$$\begin{bmatrix}\Delta P\\ \Delta Q\end{bmatrix}^n = \begin{bmatrix}H & N\\ J & L\end{bmatrix}^n \begin{bmatrix}\Delta\delta\\ \frac{\Delta V}{V}\end{bmatrix}^n \tag{31}$$

The algorithm for solving power flow problem embedded with “UPFC" is implemented for “GUPFC"[16]. The corresponding power mismatches Eqs.(34) to (39) and corresponding Jacobian elements are given in Eqs.(40) to (67).

4. Optimal location

Contingency analysis is a procedure of removing an alternator, transformer, or a transmission line for temporarily or permanently based on the requirement. Because of this the system may enter into an unstable state which may be insecure. This analysis got very importance in power system analysis to predict the contingencies so that the preventive/corrective actions can be taken appropriately. In this paper, single transmission line contingency approach is followed [29]. For each line outage, the total lines which violate the maximum power flow (OLL) and the total buses which violate the minimum/maximum voltage limits (VVB) are identified. The performance index (PI) is calculated by performing the summation of the total number of over loaded lines (NOLL) and total number of voltage violated buses (NVVB). i.e PI = NOLL + NVVB. Rank is allotted to the contingencies based on the performance index[30]. The line with highest performance index is the most severe than the remaining. Then, the shunt converter is placed at the critical bus and the two series converters are placed in the transmission lines which are connected to the critical bus and is based on the line reactance and also the line flow limits. The contingency ranking of the test system is given in Table.1.

5. Device size calculation

To get an effective and required control action, estimating proper size of GUPFC plays an important role in the present day power system FACTS device installation . Without violating loss of generality, the device power rating should be more than the device operating power in a system.

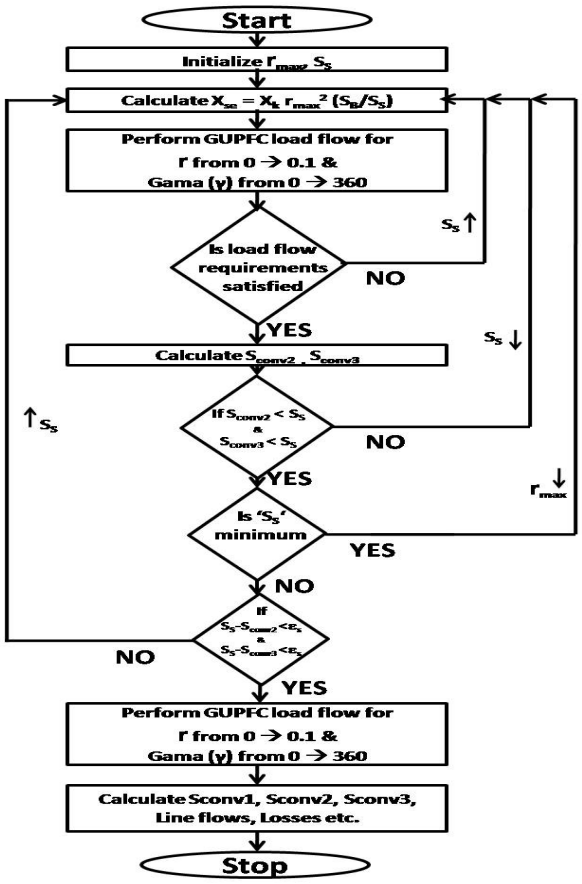

Figure 7. Flow chart to calculate device rating

Based on this principal the device rating is calculated as follows:

The reactance seen from the terminals of the series converter transformer (in p.u base on system voltage and base power) can be calculated as [6]

$$X_S = x_k r_{max}^2 \frac{\overline{S_B}}{\overline{S_S}} \tag{32}$$

where x_k is the series transformer reactance, 'r_{max}' is the factor to maximum p.u value of the injected voltage magnitude, '$\overline{S_B}$' is the system base power, and '$\overline{S_S}$' is the nominal power rating of the series converter.

Normally in transmission system, frequently used power transformers specifications are in, MVA, kV, %Z, Hz.

By using these specifications, the transformer reactance (x_k) can be calculated from the fundamentals as

$$x_k = \frac{(kV)^2 \times \%Z}{100 \times MVA}\ \Omega \tag{33}$$

Figure 7 shows the flow chart to determine the device rating.

6. Numerical results

A. Setting of the proposed approach

A MATLAB code has been developed to perform contingency analysis for finding the device location, to determine the device rating and also to analyze the effect of GUPFC on a given power system on a computer with 2.5 GHz processor and with 2GB RAM. The capability/compactness of the code can be calibrated in terms of the execution time. The time taken for each iteration with constant 'r' and 'γ' varies from 00 to 3600 with 100 interval is around 15-20 sec.

In this study, the standard Hale Network is considered to investigate the effectiveness of the proposed strategy. The data is taken from [31].

B. Illustration of contingency analysis

Table 1. Contingency analysis of test system

Line No	Outage Line	Over Loaded Lines	Line Flow/ Line Limit (MVA)	NOLL	Voltage Violated Buses	Min. Voltage Violated (p.u)	NVVB	PI=NOLL+NVVB	Rank
1	1-2	1-3	42.04/100	1	0	0	0	1	2
2	1-3	0	0	0	0	0	0	0	7
3	2-3	0	0	0	0	0	0	0	6
4	2-4	0	0	0	0	0	0	0	5
5	2-5	0	0	0	5	0.8579	1	1	1
6	3-4	0	0	0	0	0	0	0	4
7	4-5	0	0	0	0	0	0	0	3

The single line contingency analysis procedure is performed on the test system for determining the proper location and results are tabulated in Table 1. From this, it is observed that bus-5 is the critical one and the lines connected to this bus are 'line-6' and 'line-7'. Hence the device is placed in this location.

C. Optimal device rating

Based on the procedure mentioned in section 5, the device rating of the test system is calculated and are tabulated in Tables.2 with different 'Q_{sh}' values. To show the validity of the methodology, power transfoermer specifications considered in this paper are 100MVA, 138 kV, 12.7 %Z, 50 Hz. From these results, it is observed that the required nominal power rating of the converter is 10MVA.

Table 2. GUPFC rating analysis (when Q_{sh} = 0, 0.25 and 0.5 p.u)

S. No	Device Rating (MVA)	Q_{sh} = 0 p.u			Q_{sh} = 0.25 p.u			Q_{sh} = 0.5 p.u		
		$\bar{S}_S$ - M $\bar{S}_{se_1}$ (MVA)	$\bar{S}_S$ - M $\bar{S}_{se_2}$ (MVA)	Status	$\bar{S}_S$ - M $\bar{S}_{se_1}$ (MVA)	$\bar{S}_S$ - M $\bar{S}_{se_2}$ (MVA)	Status	$\bar{S}_S$ - M $\bar{S}_{se_1}$ (MVA)	$\bar{S}_S$ - M $\bar{S}_{se_2}$ (MVA)	Status
1	9	0.0223	4.15	VALID	0.0165	4.1498	VALID	0.0107	4.1496	VALID
2	10	0.0135	4.4965	VALID	0.0069	4.4962	REQUIRED	0.0004083	4.4959	REQUIRED
3	11	0.0026	4.8214	REQUIRED	-0.0047	4.8209	INVALID	-0.0119	4.8204	INVALID
4	12	-0.0103	5.125	INVALID	-0.0182	5.1243	INVALID	-0.0261	5.1236	INVALID
5	13	-0.025	5.4076	INVALID	-0.0336	5.4067	INVALID	-0.0422	5.4058	INVALID

M menas Maximum value of corresponding S_{se} as γ varies from 0^0 to 360^0

D. Analysis

This section gives the effect of device control parameters (r, γ, Q_{sh}) on a given test system. Here, the device parameters are varies as:

1. 'r' varies from 0 - 0.1 in steps of 0.02.
2. 'γ' varies from 0^0 - 360^0 in steps of 10^0.
3. 'Q_{sh}' varies from 0 - 0.5 p.u in steps of 0.25 p.u.

Table 3. Voltage magnitudes of test system under different 'Q_{sh}' values

Bus No	Voltage magnitude in p.u					
	$Q_{sh} = 0\,p.u$		$Q_{sh} = 0.25\,p.u$		$Q_{sh} = 0.50\,p.u$	
	without device ($r = 0 \& \gamma = 0^\circ$)	with device ($r = 0.1 \& \gamma = 90^\circ$)	without device ($r = 0 \& \gamma = 0^\circ$)	with device ($r = 0.1 \& \gamma = 90^\circ$)	without device ($r = 0 \& \gamma = 0^\circ$)	with device ($r = 0.1 \& \gamma = 90^\circ$)
1	1.0600	1.0600	1.0600	1.0600	1.0600	1.0600
2	1.0000	1.0000	1.0000	1.0000	1.0000	1.0000
3	0.9859	0.9860	0.9860	0.9861	0.9861	0.9861
4	0.9825	0.9826	0.9826	0.9827	0.9827	0.9828
5	0.9628	0.9632	0.9632	0.9636	0.9635	0.9640

Table 4. Active power flows through lines under different ' Q_{sh} ' values

Line No	Active power flow (MW)					
	$Q_{sh} = 0\,p.u$		$Q_{sh} = 0.25\,p.u$		$Q_{sh} = 0.50\,p.u$	
	without device ($r = 0 \,\&\, \gamma = 0^\circ$)	**with device** ($r = 0.1 \,\&\, \gamma = 90^\circ$)	**without device** ($r = 0 \,\&\, \gamma = 0^\circ$)	**with device** ($r = 0.1 \,\&\, \gamma = 90^\circ$)	**without device** ($r = 0 \,\&\, \gamma = 0^\circ$)	**with device** ($r = 0.1 \,\&\, \gamma = 90^\circ$)
1	87.7981	87.7955	87.7970	87.7945	87.7960	87.7935
2	43.4433	43.4409	43.4417	43.4393	43.4400	43.4377
3	27.0345	27.0310	27.0317	27.0283	27.0290	27.0255
4	30.9593	30.9552	30.9561	30.9520	30.9529	30.9488
5	47.3543	47.3593	47.3593	47.3643	47.3642	47.3694
6	23.4165	23.4117	23.4129	23.4081	23.4093	23.4046
7	13.7430	13.7344	13.7364	13.7278	13.7298	13.7212

Table 5. Reactive power flows through lines under different ' Q_{sh} ' values

Line No	Reactive power flow (MVAr)					
	$Q_{sh} = 0\,p.u$		$Q_{sh} = 0.25\,p.u$		$Q_{sh} = 0.50\,p.u$	
	without device ($r = 0 \,\&\, \gamma = 0^\circ$)	**with device** ($r = 0.1 \,\&\, \gamma = 90^\circ$)	**without device** ($r = 0 \,\&\, \gamma = 0^\circ$)	**with device** ($r = 0.1 \,\&\, \gamma = 90^\circ$)	**without device** ($r = 0 \,\&\, \gamma = 0^\circ$)	**with device** ($r = 0.1 \,\&\, \gamma = 90^\circ$)
1	74.4465	74.4472	74.4468	74.4475	74.4471	74.4478
2	16.9831	16.9538	16.9591	16.9299	16.9352	16.9060
3	-2.5221	-2.5590	-2.5522	-2.5890	-2.5822	-2.6191
4	-1.7460	-1.7934	-1.7847	-1.8321	-1.8233	-1.8707
5	8.5260	8.3136	8.3526	8.1404	8.1794	7.9673
6	2.4602	2.3978	2.4092	2.3469	2.3583	2.2960
7	-0.3158	-0.4242	-0.4043	-0.5127	-0.4928	-0.6011

To illustrate the effect of device on the system, 'r'=0.1 and 'γ'=90^0 is considered. The device can increase/decrease the magnitude of the voltages and angles at the buses. The Table.3 gives the effect of GUPFC, on voltage magnitude of the buses. This table reveals that, the voltage at buses varies, as 'r' varies from 0-0.1 and 'γ' varies from 0^0-20^0. The noticeable point here is that, voltage at load buses is increased after the device is placed. The voltage at bus-5 is increases drastically when Q_{sh} increases from 0-0.5 p.u at bus-5.

The corresponding power flows in the transmission lines is given in Tables.4 . It is observed from these tables is that, at constant Q_{sh}, the active and reactive power flows through some of the lines is increased/decreased.

The corresponding power flows in the transmission lines is given in Tables.4 and 5. It is observed from these tables is that, at constant Q_{sh}, the active and reactive power flows through some of the lines is increased/decreased. But, these flows in many lines gets decreased as Q_{sh} is increased.

The active and reactive power losses are given in Table.6. At constant Q_{sh}, the active and reactive power losses in the system are decreased after GUPFC is placed. But, these losses gets decreased drastically as Q_{sh} is increased.

Table 6. Active and reactive power loss in the system under different 'Q_{sh}' values

Description	$Q_{sh} = 0\,p.u$		$Q_{sh} = 0.25\,p.u$		$Q_{sh} = 0.50\,p.u$	
	Without device ($r = 0 \& \gamma = 0^\circ$)	**With device** ($r = 0.1 \& \gamma = 90^\circ$)	**Without device** ($r = 0 \& \gamma = 0^\circ$)	**With device** ($r = 0.1 \& \gamma = 90^\circ$)	**Without device** ($r = 0 \& \gamma = 0^\circ$)	**With device** ($r = 0.1 \& \gamma = 90^\circ$)
Total active power loss (MW)	6.2414	6.2390	6.2387	6.2353	6.2360	6.2327
Total reactive power loss (MVAr)	-7.7799	-8.3637	-7.7960	-8.3795	-7.8119	-8.3951

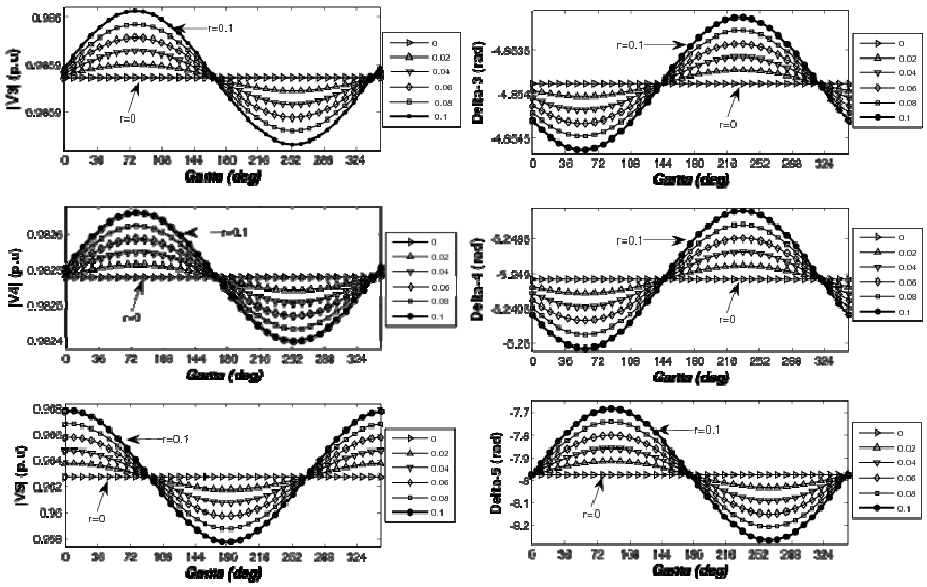

Figure 8. Voltage magnitude and phase angle variations at load buses with 'r' variation (at Q_{sh}=0)

Figure 8 shows the variation of voltage magnitudes and angles at load buses 3,4 and 5 as ' γ ' varies from 0^0 to 360^0 and ' r ' varies from '0' to '0.1' with Q_{sh} is equal to '0'. From this it is observed that there is an increase in bus voltages as ' γ ' varies from 0^0 to 90^0.

Figure 9 shows the variation of active and reactive power flows through the lines 1,5,6 and 7 as ' γ ' varies from 0^0 to 360^0 and ' r ' varies from '0' to '0.1' with Q_{sh} is equal to '0'. From this it is clear that, active power flow is increased in all lines as ' γ ' varies from 300^0 to 360^0.

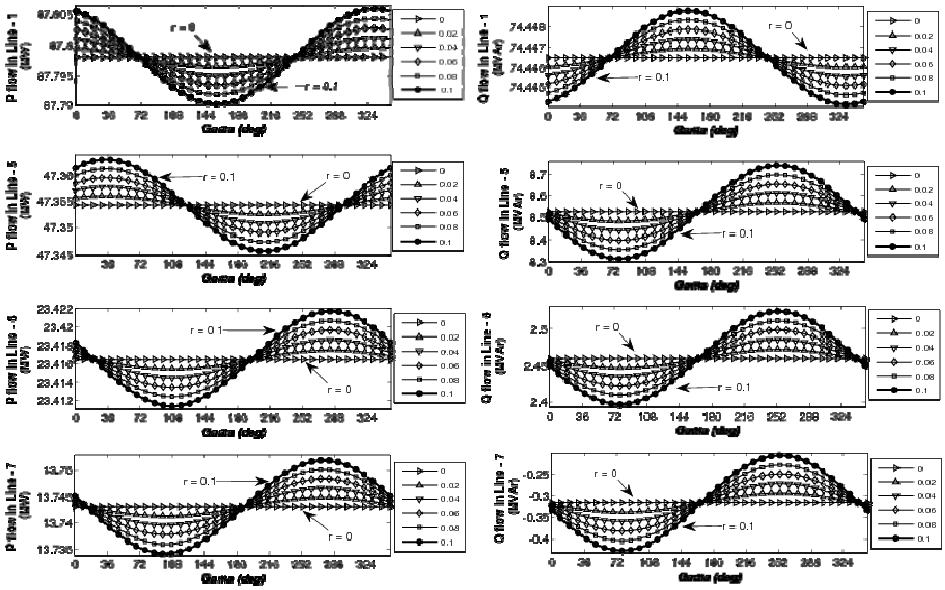

Figure 9. Active and reactive power flow variations in lines 1,3,5,7 with 'r' variation (at Q_{sh} =0)

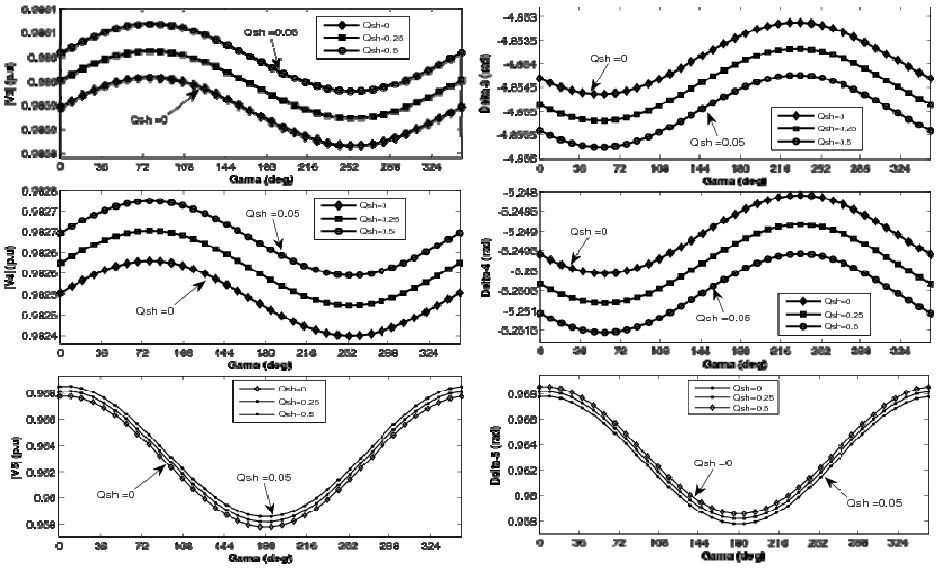

Figure 10. Voltage magnitude and phase angle variations at load buses with Q_{sh} variation (at r=0.1)

Figure 10 shows the variation of voltage magnitudes and angles at load buses 3,4 and 5 as 'γ' varies from 0^0 to 360^0 and Q_{sh} varies from '0' to '0.5'p.u with 'r' is equal to '0.1'. This shows, the bus voltage magnitude increases as 'Q_{sh}' varies from 0 to 0.05 p.u.

Figure.11 shows the variation of active and reactive power flows through the lines 1,5,6 and 7 as 'γ' varies from 0^0 to 360^0 and Q_{sh} varies from '0' to '0.5'p.u with 'r' is equal to '0.1'. This shows, the active power flow in line-5 increased as 'Q_{sh}' varies from 0 to 0.05 p.u.

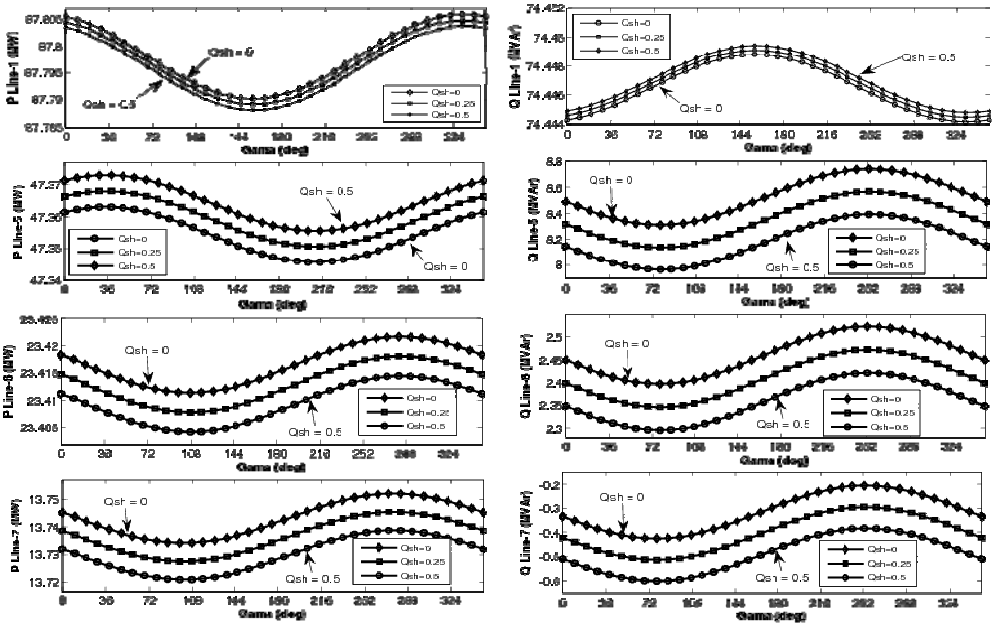

Figure 11. Active and reactive power flow variations in lines 1,3,5,7 with Q_{sh} variation (at r=0.1)

Figure 12 shows the variation of active and reactive power losses of test system as 'γ' varies from 0^0 to 360^0 and Q_{sh} varies from '0' to '0.5'p.u with 'r' is equal to '0.1'. From this it is clear that, active power and reactive power losses are decreased in the system as 'γ' varies from 40^0 to 160^0.

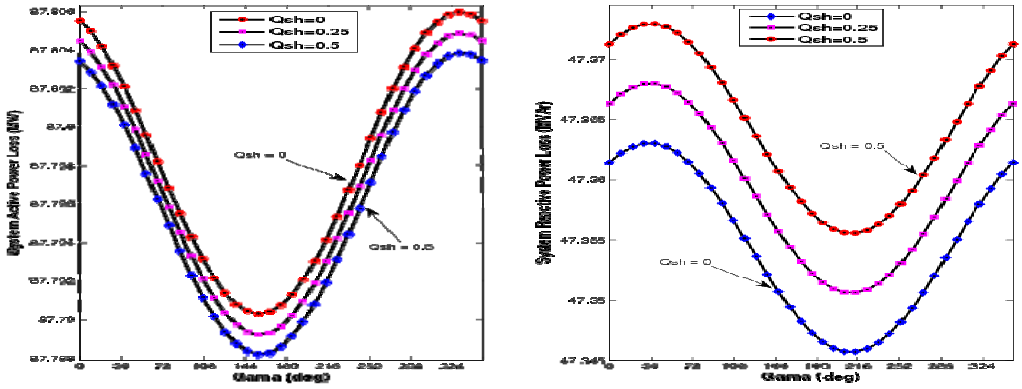

Figure 12. Active and reactive power loss variations in the system with Q_{sh} variation (at r=0.1)

Figures 13(a) and (b) shows, the variation of active and reactive power losses in the system as ' γ ' varies from 0^0 to 360^0 and ' r ' varies from '0' to '0.1' and Figures.13(c) and (d) shows, the variation of active and reactive power losses in the system as 'r' varies from '0' to '0.1' and ' γ ' is fixed at 0^0 , 90^0 , 180^0 , 270^0 with Q_{sh} is equal to '0'. From Figures. (a) and (b), it is clear that, both active and reactive power losses in the system gets decreased as ' γ ' varies from 0^0 to 160^0. From Figures. (c) and (d), it is clear that, both active and reactive power losses in the system gets decreased as ' γ ' is maintained at 90^0.

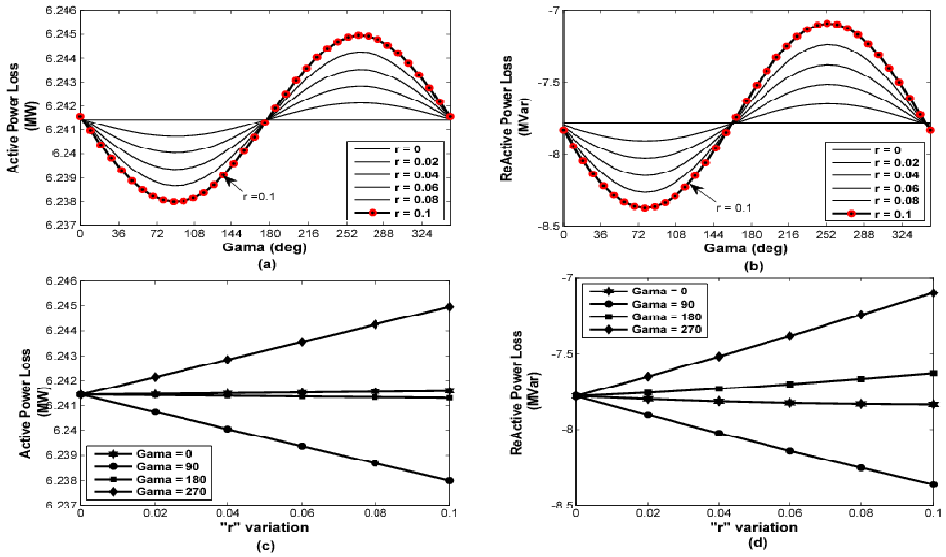

(a) and (b) with 'r' variation (c) and (d) with ' γ ' fixed at 00, 900, 1800 , 2700 (at Q_{sh} =0)

Figure 13. Active and reactive power loss variations in the system

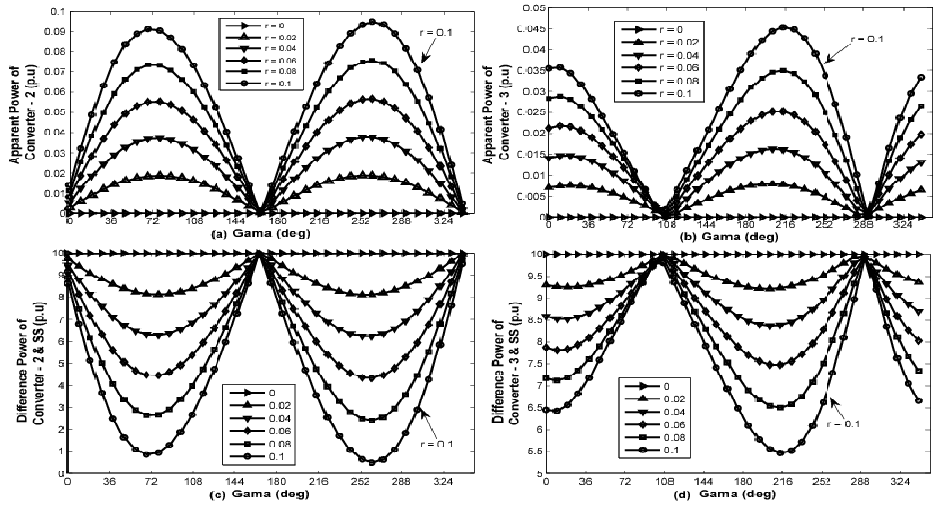

(a) and (b) with ' γ ' varies from 0^0 to 360^0 and ' r ' varies from '0' to '0.1' with Q_{sh} ='0'. (c) and (d) is the difference of converter apparent powers from the device rating.

Figure 14. Apparent power variations of the series converters

Figures 14(a) and (b) shows, the variation of apparent powers handled by the two series converters as ' γ ' varies from 0^0 to 360^0 and Figures.14(c) and (d) shows, the difference of the converter apparent powers from the device rating. Power handling capability of first converter is very nearer to the device rating (10MVA). From Figures. (a) and (b), it is clear that, when apparent power of the converter-1 is in increasing mode and simultaneously converter-2 is in decreasing mode and vice-versa.

Figure 15 shows the variation of active and reactive power flows in the transmission lines 1,5,6,7 as 'r' varies from '0' to '0.1' and ' γ ' is fixed at 0^0, 90^0 , 180^0 , 270^0 with Q_{sh} is equal to '0'.

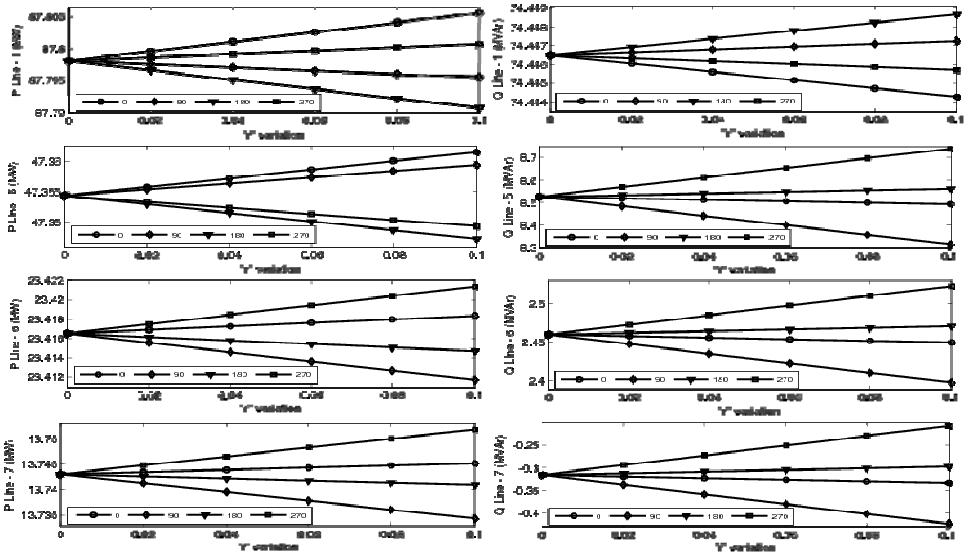

Figure 15. Active and Reactive power fow variations in the lines 1,3,5,7 with ' γ ' fixed at 0^0, 90^0 , 180^0 , 270^0 (at Q_{sh} =0)

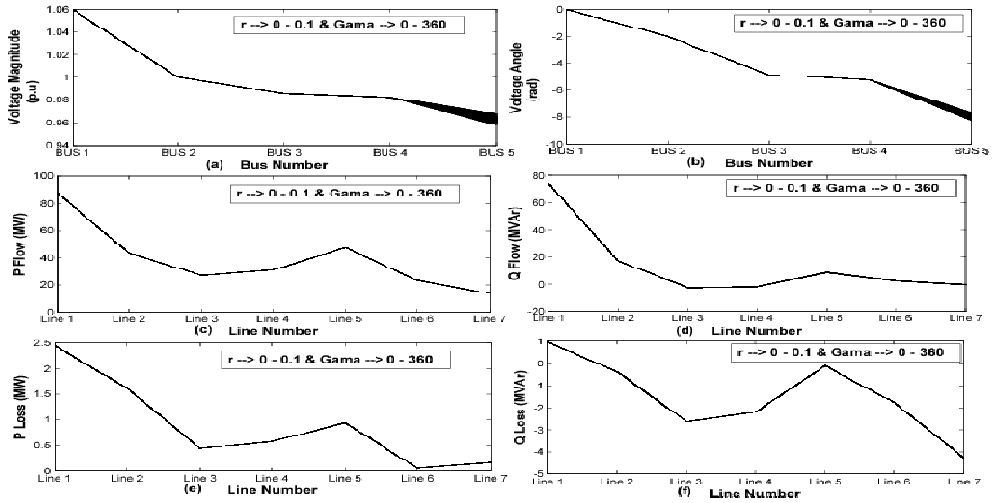

(a) and (b) are bus voltage magnitude and phase angles (c) and (d) are line active and reactive power flows (e) and (f) are system active and reactive losses

Figure 16. Variations as ' γ ' varies from 0^0 to 360^0 & ' r ' varies from '0' to '0.1' (at Q_{sh} =0)

Figure 16(a) and (b) shows the variation of the voltage magnitudes and phase angles at buses, (c) and (d) shows the active and reactive power flows in the transmission lines, (e) and (f) are active and reactive power losses in the transmission lines as ' γ ' varies from 0^0 to 360^0 and ' r ' varies from '0' to '0.1' with Q_{sh} is equal to '0'.

7. Conclusion

The effect of multi-line controller (GUPFC) has been analyzed by using the proposed Power Injection Model of the device. Since it is the combination of the multiple converters, it can simultaneously control the voltage by using shunt converter and power flows (both active and reactive) through the transmission lines using series converters. All these converters are coordinated together to perform the device operation successfully. The proposed strategies, to find optimal location and device rating works in a constrictive manner to analyze the effect of device on a given test systems. The analytical resutls shows the variation of the system parameters like, bus voltage magnitudes and phase angles, line power flows and losses greatly effects based on the device parameters like 'r', ' γ ' and ' Q_{sh} '. Finally, the developed PIM of the GUPFC can effectively controls the power system parameters of the test systems.

8. Appendices

A. Modifications in Jacobian elements

The modified diagonal and off-diagonal elements of 'H' are

$$\boldsymbol{H}'_{\boldsymbol{ii}} = \frac{\partial \boldsymbol{P}_{\boldsymbol{i},\boldsymbol{gupfc}}}{\partial \theta_{\boldsymbol{i}}} = -1.03\boldsymbol{Q}_{\boldsymbol{j},\boldsymbol{gupfc}} - 1.03\boldsymbol{Q}_{\boldsymbol{k},\boldsymbol{gupfc}} \tag{34}$$

$$H'_{ij} = \frac{\partial P_{i,gupfc}}{\partial \theta_j} = 1.03Q_{j,gupfc} \tag{35}$$

$$\boldsymbol{H}'_{\boldsymbol{ik}} = \frac{\partial \boldsymbol{P}_{\boldsymbol{i},\boldsymbol{gupfc}}}{\partial \theta_{\boldsymbol{k}}} = 1.03\boldsymbol{Q}_{\boldsymbol{k},\boldsymbol{gupfc}} \tag{36}$$

$$\boldsymbol{H}'_{\boldsymbol{jj}} = \frac{\partial \boldsymbol{P}_{\boldsymbol{j},\boldsymbol{gupfc}}}{\partial \theta_{\boldsymbol{j}}} = -\boldsymbol{Q}_{\boldsymbol{j},\boldsymbol{gupfc}} \tag{37}$$

$$\boldsymbol{H}'_{\boldsymbol{ji}} = \frac{\partial \boldsymbol{P}_{\boldsymbol{j},\boldsymbol{gupfc}}}{\partial \theta_{\boldsymbol{i}}} = \boldsymbol{Q}_{\boldsymbol{j},\boldsymbol{gupfc}} \tag{38}$$

$$\boldsymbol{H}'_{\boldsymbol{kk}} = \frac{\partial \boldsymbol{P}_{\boldsymbol{k},\boldsymbol{gupfc}}}{\partial \theta_{\boldsymbol{k}}} = -\boldsymbol{Q}_{\boldsymbol{k},\boldsymbol{gupfc}} \tag{39}$$

$$\boldsymbol{H}'_{\boldsymbol{ki}} = \frac{\partial \boldsymbol{P}_{\boldsymbol{k},\boldsymbol{gupfc}}}{\partial \theta_{\boldsymbol{i}}} = \boldsymbol{Q}_{\boldsymbol{k},\boldsymbol{gupfc}} \tag{40}$$

Simillar modification can be applied for other Jacobian elements.

B. Modifications in power mismatch equations

The modifications in active and reactive power mismatches are given as (superscript '0' indicates the power mismatches without device)

$$\Delta P_i = \Delta P_i^0 + P_{i,gupfc} \tag{41}$$

$$\Delta P_j = \Delta P_j^0 + P_{j,gupfc} \tag{42}$$

$$\Delta P_k = \Delta P_k^0 + P_{k,gupfc} \quad (43)$$

$$\Delta Q_i = \Delta Q_i^0 + Q_{i,gupfc} \quad (44)$$

$$\Delta Q_j = \Delta Q_j^0 + Q_{j,gupfc} \quad (45)$$

$$\Delta Q_k = \Delta Q_k^0 + Q_{k,gupfc} \quad (46)$$

9. System Data

The single line diagram with corresponding data of the Hale Netwrok is shown in Figure.17.

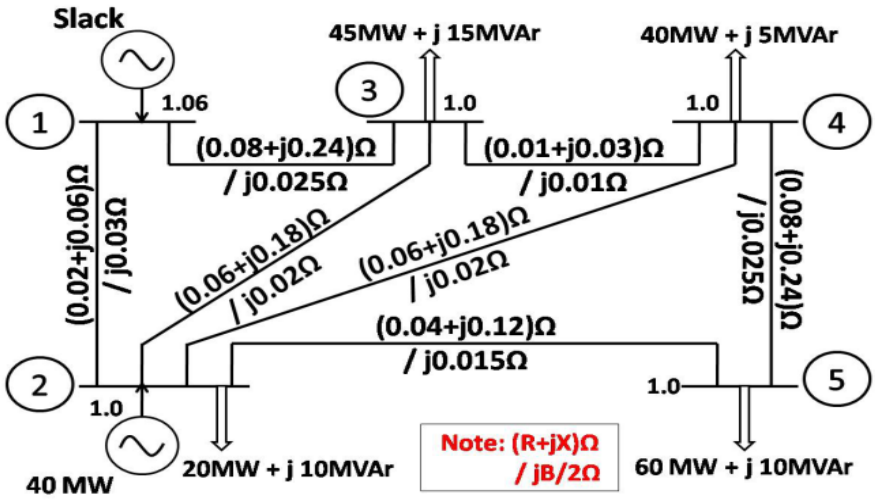

Figure 17. Hale Network

10. References

[1] N.G. Hingorani.,"Flexible AC transmission", *IEEE Spectrum* 30,1993,pp. 40-45.

[2] Xiao-Ping Zhang, Christian Rehtanz, Bikash Pal.,"*Flexible AC Transmission Systems: Modelling and Control (Power Systems)*",Springer (March 2006)., ISBN:3540306064.

[3] L. Gyugyi.,"Unified power flow control concept for Flexible AC Transmission systems", *IEE Proceedings on Generation, Transmission and Distribution*, 1992, Vol 139, No. 4, pp. 323-331.

[4] L Gyugyi, C D Schauder, et al.,"The Unified Power Flow Controller:A new appraoch to power transmission control", *IEEE Transactions on Power Delivery*, 1995, Vol. 10, No. 2, pp. 1085-1097.

[5] C R Fuerte Esquivel, E Acha.,"Unified power flow controller:a critical comparison of Newton-Raphson UPFC algorithms in power flow studies", *IEE Proceedings on Generation, Transmission and Distribution*, 1997, Vol 144, No. 5, pp. 437-444.

[6] M Noroozian, L Angquist, M Ghandhari, G Anderson.,"Use of UPFC for optimal power flow control", *IEEE Transactions on Power Delivery*, 1997, Vol. 12, No. 4, pp.1629-1634.

[7] C D Schauder, L Gyugyi, M R Lund, et al.,"Operation of the Unified Power Flow Controller (UPFC) under practical constraints", *IEEE Transactions on Power Delivery*, 1998, Vol 13, No. 2, pp. 630-639.

[8] A J F Keri, A S Mehraban., et al., "Unified Power Flow Controller(UPFC):Modeling and Analysis", *IEEE Transactions on Power Delivery*, 1999, Vol 14, No. 2, pp. 648-654.

[9] B A Renz, A Keri, et al.,"AEP Unified Power Flow Controller Performance", *IEEE Transactions on Power Delivery*, 1999, Vol. 14, No. 4, pp. 1374-1381.

[10] C R Fuerte Esquivel, E Acha, H Ambriz Perez.,“A Comprehensice Newton-Raphson UPFC Model for the Quadratic Power Flow Solution of Practical Power Networks", *IEEE Transactions on power systems*, 2000, Vol. 15, No. 1, pp. 102-109.
[11] Wanliang Fang, H W Ngan.,“A robust load flow technique for use in power system with unified power flow controller", *Electric Power Systems Reseach*., 2000, Vol 53, pp. 181-186.
[12] K S Verma, S N Singh, H O Gupta.,“Location of unified power flow controller for congestion management", *Electrical Power and Energy Systems*, 2001, Vol. 58, pp. 89-86.
[13] D Z Fang, Z Fang, H F Wang.,“Application of the injection modeling approach to power flow analysis for systems with unified power flow controller", *Electrical Power and Energy Systems*, 2001, Vol. 23, pp. 421-425.
[14] A. L Abbate, M. Trovato, C. Becker, E. Handschin.,“Advanced Steady-State Model of UPFC for Power System Studies", *Power Engineering Society Summer Meeting (IEEE)*, 2002, Vol. 1, pp 449-454.
[15] M H Haque, C M Yam.,“A simple method of solving the controlled load flow problem of a power system in the presence of UPFC", *Electric Power Systems Reseach*., 2003, Vol 65, pp. 55-62.
[16] Mehmet Tumay, A M Vural, K L Lo.,“The effect of unified power flow controller location in power systems", *Elecrical Power and Energy Systems*, 2004, Vol. 26, pp. 561-569.
[17] A Mete Vural, Mehmet Tumay.,“Mathematical modeling and analysis of a unified power flow controller: A comparision of two appraoches in power flow studies and effects of UPFC location", *Electrical Power and Energy Systems*, 2007, Vol. 29, pp. 617-629.
[18] Suman Bhowmick, Biswarup Das, Narendra Kumar.,“An Indirect UPFC Model to Enhance Reusability of Newton Power Flow Codes", *IEEE Transactions on Power Delivery*, 2008, Vol. 23, No. 4, pp. 2079-2088.
[19] B. Fardanesh, B. Shperling, E. Uzunovic, S.Zelingher.,“Multi-Converter FACTS Devices:The Generalized Unified Power Flow Controller (GUPFC)", *Power Engineering Society Summer Meeting, 2000. IEEE*., Vol. 2, pp. 1020-1025.
[20] Xiao-Ping Zhang, Edmund Handschin, Maojun Mike Yao.,“Modeling of the Generalized Unified Power Flow Controller (GUPFC) in a Nonlinear Interior Point OPF", *IEEE Transactions on Power Systems*, Vol 16, No. 3, 2001, pp 367-373.
[21] X P Zhang.,“Modelling of the interline power flow controller and the generalised unified power flow controller in Newton power flow", *IEE Proceedings on Generation, Transmission and Distribution*, 2003, Vol 150, No. 3, pp. 268-274.
[22] Lin Sun Shengwei Mei, Qiang Lu, Jin Ma.,“Application of GUPFC in Chinaâ€™s Sichuan Power Grid-Modeling, Control Strategy and Case Study", *Power Engineering Society General Meeting (IEEE)*, 2003, Vol. 1, pp. 175-181.
[23] Sheng-Huei Lee, Chia-Chi Chu.,“Power Flow Computations of Convertible Static Compensators for Large-Scale Power Systems", *Power Engineering Society General Meeting (IEEE)*, 2004, Vol. 1, pp. 1172-1177.
[24] X P Zhang.,“Robust modeling of the interline power flow controller and the generalized unified power flow controller with small impedances in power flow analysis", Electrical *Engineering (Springer Verlag)*, 2006, Vol.89, pp. 1-9.
[25] J G Singh, P Tripathy, S N Singh, C Srivastava.,“Development of a fuzzy rule based generalized unified power flow controller", *European Transactions on Electrical Power*, 2009, Vol.19, pp. 702-717.
[26] Rakhmad Syafutra Lubis, Sasongko Pramono Hadi, Tumiran.,“Modeling of the Generalized Unified Power Flow Controller for Optimal Power Flow", *ICEEI (IEEE)*, 2011, pp. 1-6.
[27] Rakhmad Syafutra Lubis., “Modeling and Simulation of Generalized Unified Power Flow Controller (GUPFC)", *2nd International Conference on ICICI-BME (IEEE)*, 2011., pp. 207-213.

[28] R Thirumalaivasan, Nagesh Prabhu, M Janaki, D P Kothari.,"Analysis of subsynchronous resonance with generalized unified power flow controller", *Electrical Power and Energy Systems*, 2013, Vol.53, pp. 623-631.
[29] H I Shaheen, G I Rashed, S J Cheng.,"Optimal Location and Parameters Setting of UPFC based in GA and PSO for Enhancing Power System Security under Single Contingencies", *Power and Energy Society General Meeting - Conversion and Delivery of Electrical Energy in the 21st Century (IEEE)*, 2008, pp. 1-8.
[30] Iman Ziari, Alireza Jalilian.,"Optimal placement and sizing of multiple APLCs using a modified PSO", *Electrical Power and Energy Systems*, 2012, Vol. 43, pp. 630-639.
[31] Stagg N G, El-Abiad H A.,"*Computer Methods in Power System Analysis*", McGraw-Hill Inc., 1968.

Chintalapudi Venkata Suresh (Non-member) is currently pursuing Ph.D. in the department of Electrical and Electronics Engineering, University College of Engineering Kakinada, Jawaharlal Nehru Technological University Kakinada, Kakinada, A.P., India. His interests include, Computer Applications in Power Systems, Optimization Techniques, FACTS, Power System Analysis including FACTS devices and Power System Operation and Control.

Sirigiri Sivanaga Raju (Non-member) is Professor in the department of Electrical and Electronics Engineering, University College of Engineering Kakinada, Jawaharlal Nehru Technological University Kakinada, Kakinada, A.P., India. He completed his Master's degree from Indian Institute of Technology, Khargpur, India, in electrical power systems. He completed his doctoral program from Jawaharlal Nehru Technological University Hyderabad, Andhra Pradesh, India. His interests include FACTS Controllers, Electrical Distribution System Automation, Optimization Techniques, Voltage Stability, Power System Analysis, and Power System Operation and Control.